Inorganica Chimica Acta, 125 (1986) 135–142

Spectroelectrochemistry of a Urea-linked Oxo-bridged Iron Porphyrin Dimer

LAWRENCE A. BOTTOMLEY*, JEAN-NOEL GORCE

School of Chemistry, Georgia Institute of Technology, Atlanta, Ga. 30332, U.S.A.

and JOHN T. LANDRUM

Department of Physical Sciences, Florida International University, Miami, Fla. 33199, U.S.A.

(Received March 17, 1986)

Abstract

The electrochemical behavior of μ-oxo-*N,N*-bis-(5-(*o*-phenyl)-10,15,20-triphenylporphinatoiron(III))–urea mono hydrate, $[(FF)Fe]_2O$, was investigated at a platinum electrode in both 1,2-dichloroethane and pyridine. In $EtCl_2$, electroreduction of this oxo-bridged and urea-linked dimer produced a binuclear ferrous hydroxide porphyrin. This latter species could be oxidized to regenerate the μ-oxo dimer in quantitative yield. In pyridine, $[(FF)Fe]_2O$ underwent a chemically irreversible electroreduction producing a hexacoordinate binuclear ferrous porphyrin with pyridine occupying the axial positions of each iron atom. Oxidation of this species also produced the μ-oxo and urea-linked dimer in quantitative yield. These results are in contrast to the redox behavior of $[(TPP)Fe]_2O$ in these solvents. Electron transfer pathways, consistent with voltammetric and spectroelectrochemical results, are proposed for $[(FF)Fe]_2O$ and compared with those found for $[(TPP)Fe]_2O$. The redox behavior observed for $[(FF)Fe]_2O$ implicates the steric constraint of the urea linkage and hydrogen bonding of the protonated bridging oxygen atom with the amide groups. This marks the first evidence of molecular environmental effects in the redox chemistry of hematin dimers.

Introduction

During the last ten years, a number of porphyrins have been synthesized with steric superstructures located on one side of the porphyrin. These 'picket fence' [1], 'capped' [2], 'cyclophane' [3], 'pocket' [4], 'crowned' [5], 'strapped' [6] and 'basket-handled' [7] porphyrins were prepared in an attempt to mimic the reversible uptake of dioxygen by hemoproteins. The complexes cited were also successful, to varying degrees, in prohibiting the oxidation of the ferrous dioxygen complexes to the μ-oxo dimer.

In many of the above complexes, the steric superstructures were bound to the porphyrin via either amide or ether linkages. There is compelling evidence that the selection of the linking moiety significantly impacts the physicochemical properties of the porphyrin. NMR studies have shown that the amide linkage stabilizes the dioxygen adduct as compared to the ether linkage via distal polar interactions [8]. These studies also demonstrated the formation of an H bond between the NHCO linkage and the coordinated dioxygen. Recently, Lexa and coworkers [9] have shown that the identity of the linking group for the 'basket-handled' porphyrins exerted a pronounced influence on both the electrochemistry and ligand binding properties of the iron derivatives. These authors have also demonstrated that the choice of the linking moiety determined whether the oxidation of Cu, Zn or Mg 'basket-handled' porphyrins occurred in two discrete, one electron transfer steps or in a single two electron step.

We found the discovery of a single two electron oxidation of the amide-linked 'basket-handled' metalloporphyrins intriguing. There are only a few examples in the literature where changes in the metalloporphyrin substituent produced a change in the number of electrons involved in the charge transfer step [10–12]. Landrum and coworkers [13] have previously characterized a urea-linked tetraphenylporphyrin dimer with a μ-oxo bridge between two Fe(III) centers (abbreviated as $[(FF)Fe]_2O$ and depicted in Fig. 1). The possibility that the urea-linkage might produce redox reactivity comparable to that observed for the amide-linked 'basket-handled' porphyrin prompted this investigation.

Experimental

Materials

$[(FF)Fe]_2O$ was synthesized as previously reported [13]. The μ-oxo dimer was cleaved by successive

* Author to whom correspondence should be addressed.

0020-1693/86/$3.50

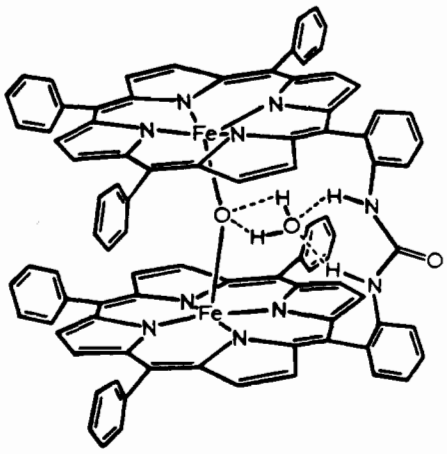

[(FF)Fe]$_2$O

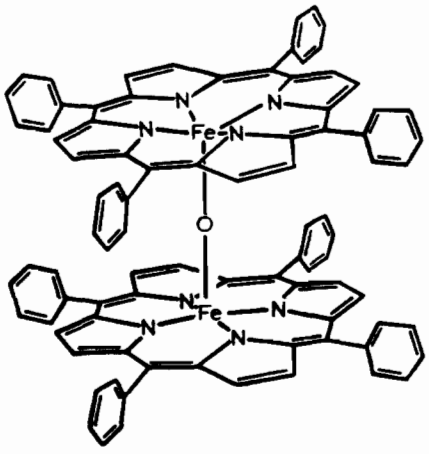

[(TPP)Fe]$_2$O

Fig. 1. Structures of [(FF)Fe]$_2$O and [(TPP)Fe]$_2$O.

extractions of a dichloromethane solution of [(FF)-Fe]$_2$O with equal volumes of 2 M aqueous HCl to form the urea-linked ferric chloride binuclear porphyrin complex, [(FF)FeCl]$_2$. The μ-oxo dimer of iron tetraphenylporphyrin (abbreviated as [(TPP)-Fe]$_2$O) was prepared by the method of Adler and coworkers [14].

The supporting electrolyte, tetrabutylammonium perchlorate, TBAP, was obtained from the Eastman Chemical Co. Prior to use, TBAP was recrystallized three times from absolute ethanol, vacuum dried for 24 h and stored in an evacuated desiccator. 1,2-dichloroethane, $EtCl_2$, was extracted successively from concentrated sulfuric acid and distilled, deionized water. The resultant extract was fractionally distilled over phosphorous pentoxide in a nitrogen atmosphere and stored in the dark over activated 4 Å molecular sieves. Pyridine was stored over potassium hydroxide. Prior to use, it was fractionally distilled over calcium oxide under a nitrogen atmosphere.

Instrumentation

Visible spectral measurements were obtained with a Tracor Northern 6050 spectrometer in conjunction with the Tracor Northern 1710 multichannel analyser. Data output was to either a dual Data Systems Design floppy disk storage device or directly to a Hewlett Packard 7470A Graphics Plotter. Specifications for this system have previously been reported [15].

Cyclic voltammetric experiments were carried out on an IBM Instruments, Inc., Model EC225 polarographic system. A conventional three-electrode system was used with a Pt-button working electrode, a Pt-wire counter electrode and a saturated calomel electrode (SCE) as reference. Aqueous contamination of electrochemical solutions from the reference electrode was minimized by isolating the reference electrode via a frit. Voltammograms obtained at a scan rate of 20 to 500 mV s^{-1} were recorded on a Houston Omnigraphic 2000 X–Y recorder. Voltammograms recorded at scan rates faster than 500 mV s^{-1} were recorded on a Type 564 Storage Oscilloscope equipped with two Type 3472 Dual Trace Amplifiers. To compensate for solution resistence, positive feedback IR compensation was employed.

Differential pulse voltammograms were performed on the IBM instrument modified to allow the user to select the pulse direction independently of the potential sweep direction. For the differential pulse experiments, a potential scan rate of 10 mV s^{-1} was used. The pulse interval was maintained at 0.1 s while pulse amplitudes varied between 5 and 100 mV.

All solutions were deoxygenated by passing a stream of solvent saturated prepurified nitrogen into the solution for at least 10 min prior to recording voltammetric data. To maintain an oxygen free environment, the solution was blanketed with nitrogen during all experiments. All potentials reported herein were referenced to the SCE and were not corrected for liquid junction potentials.

Results and Discussion

Voltammetry of [(FF)Fe]$_2$O in $EtCl_2$

In the non-bonding solvent, $EtCl_2$, [(FF)Fe]$_2$O underwent four electrooxidations and one electroreduction processes. A typical steady state cyclic voltammogram and a differential pulse voltammogram depicting these charge transfer reactions are shown in Fig. 2. A variable potential sweep rate experiment was carried out on the reduction process. The pertinent results were: (a) $i_{p,a}/i_{p,c}$ remains unity

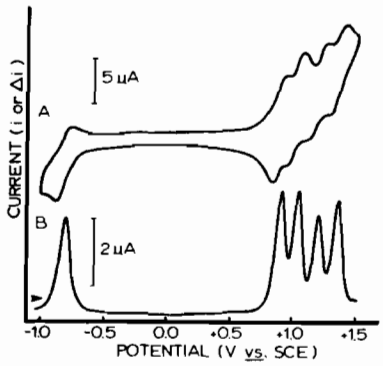

Fig. 2. Voltammetric data obtained on a 1.29 mM solution of $[(FF)Fe]_2O$ in $EtCl_2$. Trace A is a steady state cyclic voltammogram taken at a potential sweep rate of 200 mV s^{-1}. Trace B is a differential pulse voltammogram taken at a potential sweep rate of 10 mV s^{-1}, a pulse amplitude of 25 mV and a pulse frequency of 0.1 s. Note that the oxidative currents are positive.

regardless of the scan rate; (b) $E_{1/2}$ is consistently –0.90 V and $E_{p/2}$ is consistently –0.87 V at all scan rates; (c) at 500 mV s^{-1}, $E_{p,a} - E_{p,c} = 89$ mV and decreases to 60 mV at 20 mV s^{-1}; (d) the forward peak current, $i_{p,a}$, is directly proportional to the square root of the scan rate, $V^{1/2}$ and (e) at 20 mV s^{-1}, $E_{p,a} - E_{p,c}$ and $E_{p,a} - E_{1/2}$ are 58 and 30 mV respectively. Differential pulse voltammograms were also obtained for this charge transfer reaction at various pulse heights and pulse directions. Analysis of these data as per the method of Birke [16] showed that (a) $E_{p(-)} - E_{p(+)}$ to be within 1 mV of the pulse amplitude; (b) $i_{p(+)}/i_{p(-)}$ to be slightly less than unity; and (c) $W_{1/2}$ was linearly related to the pulse amplitude. Extrapolation to a pulse amplitude of 0 mV yielded a $W_{1/2}$ value of 91 mV. Taken collectively, the voltammetric data indicated that the reduction process is best described as a one electron quasi-reversible electron transfer.

Variable potential sweep rate experiments were carried out on the oxidation processes and analyzed as above. Midpoint potentials were invariant with potential sweep rate and were observed at 0.91, 1.05, 1.29 and 1.43 V, respectively. At a sweep rate of 20 mV/s, the peak potential separation ($E_{p,a} - E_{p,c}$) was 70 ± 5 mV for each process and increased with increasing sweep rates. Due to the highly overlapping peaks, the cyclic voltammetric peak current dependence on potential sweep rate was analyzed only for the first oxidation process. The anodic peak current was proportional to $V^{1/2}$ and equal in magnitude to the current observed on the cathodic sweep.

Differential pulse voltammograms were obtained for all four oxidations over the pulse amplitudes of ±5 to ±100 mV. These data were analyzed as per the method of Birke [16] and gave results comparable to those described above for the reduction process. Taken collectively, these data indicated that the oxidation of $[(FF)Fe]_2O$ is best described as four sequential one electron quasi-reversible charge transfers.

Controlled potential coulometry on a solution of $[(FF)Fe]_2O$ was performed to determine the total number of electrons involved in each charge transfer reaction. Stepping the potential from +0.70 to +1.00 V resulted in one equivalent of charge being transferred per dimer. Increasing the applied potential to 1.16 V resulted in an additional transfer of one equivalent of charge. Reversing the applied potential to +1.00 V and then to +0.70 V resulted in the sequential passage of two equivalents per dimer and confirmed the chemical reversibility of the first two oxidation steps.

Spectroelectrochemistry of $[(FF)Fe]_2O$ in $EtCl_2$

To ascertain the long term stability of the reduction and oxidation products, potentiostatic chronoabsorptometric experiments were performed. A 1.54×10^{-4} M solution was placed in an optically transparent thin-layer electrochemical cell. Over the potential range of 0.75 to –0.75 V, a stable electronic spectrum characteristic of $[(FF)Fe]_2O$ was observed. The spectrum possessed an intense Soret band at 410 nm and two visible bands at 572 and 612 nm. Upon stepping the potential from the E_{oc} to 1.00 V, the first oxidation step was initiated and changes in the electronic spectrum were recorded. An unchanging spectrum was obtained within 70 s. During the course of the spectroelectrochemical transition, the Soret band underwent a 25% reduction in intensity without a shift in wavelength. The alpha band disappeared while the beta band lost intensity but did not shift. Isosbestic points were observed at 392, 467, 565 and 580 nm. This spectral interconversion is depicted in the upper portion of Fig. 3. The lower portion of Fig. 3 depicts the spectral changes observed after stepping the electrode potential to 1.20 V. During the electrogeneration of the dimer dication, the visible band disappeared and the Soret band lost 56% of its intensity, shifting to 430 nm. The spectral interconversion was complete within 70 s and was accompanied by isosbestic points at 371 and 430 nm. Reversal of the potential to 1.00 V regenerated 98% of the first oxidation product as judged by the intensity of the Soret band. Reversal of the applied potential to 0.75 V regenerated 97% of the starting material.

The spectroelectrochemical findings concur with the voltammetric results and indicate that electrooxidation of $[(FF)Fe]_2O$ proceeds quasi-reversibly as described in eqns. 1–4.

$$[(FF)Fe]_2O \overset{0.91\,V}{\rightleftharpoons} \{[(FF)Fe]_2O\}^+ + e^- \quad (1)$$

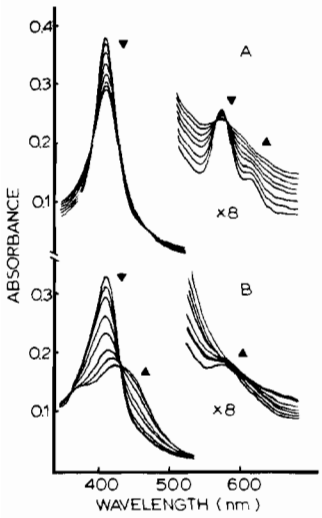

Fig. 3. Electronic spectra obtained during the electrooxidation of a 0.540 mM solution of $[(FF)Fe]_2O$ in $EtCl_2$. Part A depicts the spectra obtained when the applied potential was stepped from E_{oc} to 1.00 V. Part B depicts the spectra obtained when the applied potential was stepped from 1.00 to 1.20 V. Spectra were acquired every 10 s.

TABLE I. Midpoint Potentials: $[(TPP)Fe]_2O$ and $[(FF)Fe]_2O$ in $EtCl_2$

Compound	Redox couple				
	+3/+4	+3/+2	+2/+1	+1/0	0/−1
$[(FF)Fe]_2O$	1.40	1.29	1.05	0.91	−0.90
$[(TPP)Fe]_2O$	1.38	1.32	1.00	0.78	−1.01

$$\{[(FF)Fe]_2O\}^{+} \overset{1.05\,V}{\rightleftharpoons} \{[(FF)Fe]_2O\}^{+2} + e^{-} \quad (2)$$

$$\{[(FF)Fe]_2O\}^{+2} \overset{1.29\,V}{\rightleftharpoons} \{[(FF)Fe]_2O\}^{+3} + e^{-} \quad (3)$$

$$\{[(FF)Fe]_2O\}^{+3} \overset{1.43\,V}{\rightleftharpoons} \{[(FF)Fe]_2O\}^{+4} + e^{-} \quad (4)$$

The observation of four chemically reversible electrooxidations for μ-oxo iron porphyrin dimers was only recently reported [10]. Comparison of the half wave potentials observed for $[(FF)Fe]_2O$ with those observed for $[(TPP)Fe]_2O$ in $EtCl_2$ (see Table I) indicates that the urea-linked oxo dimer is more difficult to oxidize by 130 mV. The first two oxidations of the $[(FF)Fe]_2O$ complex are shifted anodically, indicating a preferential stabilization of the dimeric species with the lower charge by the urea linkage. Lexa and coworkers [9] have recently reported the electroreduction of several amide-linked basket handle and picket fence iron porphyrin derivatives. For all of the complexes studied, the half wave potentials for the Fe(III) to Fe(II), the Fe(II) to Fe(I) and the Fe(I) to porphyrin anion radical charge transfer steps were anodic with respect to the comparable charge transfer reactions for the TPP derivative. This trend cannot be a result of the inductive effects of the phenyl ring substituent because the Hammett–Taft substituent constant for the amide moiety is not appreciably different from that of a hydrogen atom [17]. The authors [9] suggested that hydrogen bonding by the amide hydrogen and/or dipole-charge interactions might be responsible for the stabilization of the negatively charged species. Our results indicated a similar trend for the electrooxidation of $[(FF)Fe]_2O$.

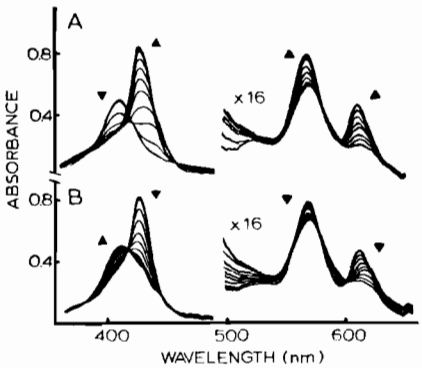

Fig. 4. Electronic spectra obtained during the electroreduction of a 0.200 mM solution of $[(FF)Fe]_2O$ in $EtCl_2$. Part A depicts the spectra obtained when the applied potential was stepped from −0.75 to −1.05 V. No spectral changes were observed when the potential was stepped back from −1.05 to −0.75 V. Part B depicts spectra obtained when the applied potential was stepped from −0.75 to −0.40 V Spectra were acquired every 20 s.

The reduction of $[(FF)Fe]_2O$ in $EtCl_2$ was also investigated spectroelectrochemically. Stepping the potential from −0.75 to −1.05 V resulted in the spectral changes depicted in Fig. 4. The Soret band at 410 nm decreased while a new band at 426 nm increased to an intensity 1.7 times that of the original. Both the alpha and the beta bands increased in intensity and shifted to 607 and 565 nm, respectively. A low intensity visible band grew at 526 nm. The final spectrum was obtained within 160 s after the application of the potential (−1.05 V). Well defined isosbestic points were not observed throughout this electrolysis. Initially (from zero to 50 s after application of the reducing potential) isosbestic points were observed at 390, 421, 460, 540, 577, 594 and 631 nm. At this point in time, the spectral conversions were devoid of isosbestic points until the last 50 s of the electrolysis. Over this time interval, spectral transitions were characterized by isosbestic points at 375, 414, 441, 514, 578, 595 and 615 nm. Upon stepping the potential back to −0.75 V, no spectral changes were observed. However, when the applied potential was increased to −0.40 V, spec-

TABLE II. Spectral Data for $[(TPP)Fe]_2O$ and $[(FF)Fe]_2O$

Compound	Solvent	Product[a]	Absorption maxima (nm)			Extinction coefficient (×100 000)		
$[(FF)Fe]_2O$	$EtCl_2$	0	410	572	612	1.37	0.11	0.07
		+1	410	572		1.06	0.11	
		+2	430			0.60		
	Pyridine	0	413	572	611	1.35	0.13	0.05
		−1[b]	425	533	563	2.15	0.30	0.11
$[(TPP)Fe]_2O$	$EtCl_2$	0	407	572	613	1.32	0.11	0.05
		+1	409	574	688	1.08	0.10	0.05
		+2	392	445	554	0.78	0.42	0.03
	Pyridine	0	410	573	614	1.35	0.11	0.05
		−1[b]	424	530	612	2.30	0.31	0.07

[a]Charge on the dimer. [b]Decomposition product.

tral changes were immediately observed. The 426 nm Soret band decreased while a new one at 412 nm appeared. Both the alpha and the beta bands lost intensity while red shifting to 609 and 568 nm, respectively. A stable spectrum was obtained in 180 s and had been produced with isosbestic points at 383, 417, 456, 577, 597 and 616 nm. In this spectrum the Soret was contaminated by two small shoulders at 427 and 441 nm. However at an applied potential of 0.0 V these disappeared and a spectrum identical to that of the starting material was obtained within 40 s.

Bulk electrolysis at an applied potential of −1.10 V resulted in the passage of 1.86 ± 0.15 electrons per dimer, in apparent conflict with the voltammetric results. Stepping the potential back to −0.75 V resulted in the passage of capacitance current only, indicating that a chemically irreversible reduction of the dimer had occurred at −1.10 V. The spectrum of the final reduction product is remarkably similar to that observed by Kadish *et al.* [18] for $\{(TPP)FeOH\}^-$ in dimethylformamide and to that of Lexa *et al.* [9c] for the Fe(II)–hydroxy complex of the 'basket-handled' porphyrin in benzonitrile. Complete regeneration of the dimer was observed after stepping the electrode potential to values anodic of −0.40 V. Taken collectively, the voltammetric, coulometric and spectroelectrochemical results indicated that electroreduction of $[(FF)Fe]_2O$ proceeded via an ECE mechanism with the second electron transfer occurring at $E_{1/2} \geqslant -0.89$ V and linked to the first via a relatively slow chemical reaction as proposed in eqns. (5)–(8).

$$[(FF)Fe^{III}]_2O + e^- \rightleftharpoons \{[(FF)Fe^{II}]-O-[(FF)Fe^{III}]\}^- \quad (5)$$

$$\{[(FF)Fe^{II}]-O-[(FF)Fe^{III}]\}^- + e^- \xrightarrow{H_2O} \{[(FF)Fe^{II}(OH)]_2\}^{2-} \quad (6)$$

$$\{[(FF)Fe^{II}(OH)]_2\}^{2-} \longrightarrow [(FF)Fe^{III}(OH)]_2 + 2e^- \quad (7)$$

$$[(FF)Fe^{III}OH]_2 \longrightarrow [(FF)Fe^{III}]_2O + H_2O \quad (8)$$

Although a number of workers have investigated the electrochemistry of $[(TPP)Fe]_2O$ in a variety of nonaqueous solvents [18–23] the electroreduction pathway has not been detailed in this medium. Comparative experiments were carried out on $[(TPP)Fe]_2O$ to evaluate the influence of the urea-linkage on the rate of the following chemical reaction. Variable potential sweep rate experiments indicated that $[(TPP)Fe]_2O$ underwent a one electron reduction at $E_{1/2} = -1.01$ V in $EtCl_2$. This species was characterized by a Soret band at 410 nm and two visible bands at 572 and 612 nm. Upon applying a potential of −1.15 V, the following spectral changes occurred: (a) within the first 30 s the Soret lost 3% of its intensity while the visible bands remained intact; no shifts in wavelength were observed; (b) the spectrum remained with no further spectral changes for 180 s after which time a shoulder developed at 433 nm; (c) After 3 min a stable spectrum was obtained characterized by a Soret at 410 nm which was 90% of the initial Soret, a second low intensity Soret at 435 nm and two visible bands and 572 and 612 nm. In contrast to $[(FF)Fe]_2O$, reversing the applied potential to −0.85 V completely regenerated the spectrum of $[(TPP)Fe]_2O$ within 2 min.

The combined voltammetric and spectroelectrochemical results confirmed that electroreduction of $[(TPP)Fe]_2O$ also proceeds via an ECE mechanism. However, the rate of the chemical reaction linking the two electron transfers is considerably slower. In an attempt to enhance the rate, aliquots of water were added to a solution of $[(TPP)Fe]_2O$. Cyclic voltammograms taken on solutions containing from zero equivalents to solutions which were completely saturated with water did not show any changes in the

reversibility of the electroreduction process. A potentiostatic spectroelectrochemical experiment on a solution of $[(TPP)Fe]_2O$ with 5 equivalents of water gave results identical to those observed in the absence of added water. In a solution saturated with water, the electroreduction of $[(TPP)Fe]_2O$ resulted in the formation of monomeric (TPP)Fe which could not be subsequently converted to the dimer. The observed reactivity parallels that previously reported by Jones *et al.* [21] for this dimer in dimethylsulfoxide, dimethylformamide and pyridine.

Voltammetry of $[(FF)Fe]_2O$ in Pyridine

$[(FF)Fe]_2O$ was electroinactive in pyridine over the potential range +1.30 to −0.60 V. An electroreduction was observed at $E_{p,c} = -0.71$ V (at $V = 200$ mV/s). This charge transfer reaction was coupled to an oxidation at $E_{p,a} = 0.14$ V (at $V = 200$ mV/s). Variable potential sweep rate studies on the cathodic process revealed the following trends: (a) $E_{p,c}$ shifted by −29 mV per ten-fold increase in scan rate over the potential sweep range $0.01 \leqslant V \leqslant 9.90$ V/s; (b) $i_{p,c}/V^{1/2}$ ratios decreased as a function of increasing scan rate; (c) $E_{p,c/2} - E_{p,c}$ was 78 mV at a scan rate of 20 mV s^{-1} and decreased with increasing scan rate. At scan rates greater than 1.0 V s^{-1}, a corresponding anodic process was observed at $E_{p,a} = -0.62$ V. The ratio of $i_{p,a}/i_{p,c}$ was less than unity and increased with increasing sweep rate. Similarly, variable potential sweep rate studies on the anodic process at 0.14 V revealed that: (a) $E_{p,a}$ shifted by −20 mV per ten-fold increase in scan rate; (b) $i_{p,a}/V^{1/2}$ ratios decreased as a function of increasing scan rate and (c) $E_{p,a/2} - E_{p,a}$ was 88 mV at a scan rate of 20 mV s^{-1} and decreased with increasing scan rate. Steady state voltammograms taken at scan rates less than 2.0 V/s indicated complete regeneration of $[(FF)Fe]_2O$ after the oxidation. At scan rates equal to or greater than 2.0 V/s, redox couples were observed for both processes as depicted in Fig. 5.

To evaluate the role of pyridine in the electron transfer sequence, three separate experiments were performed. In the first experiment, aliquots of pyridine were added to a solution of $[(FF)Fe]_2O$ dissolved in neat $EtCl_2$. The initial reduction remained reversible (at $E_{1/2} = -0.90$ V) up to 5.0 eq of pyridine. At [py] > 5.0 eq, the anodic process at $E_{p,a} = -0.86$ V decreased in amplitude. A new anodic process grew in intensity at $E_{p,a} = 0.14$ V and $E_{p,c}$ shifted from −0.94 to −0.71 V. At 500 eq of pyridine, the voltammetric behavior of $[(FF)Fe]_2O$ was similar to that observed in neat pyridine. These results implicated coordination of pyridine to the reduction product electrochemically generated at −0.71 V.

In a second experiment, the urea-linked binuclear ferric porphyrin complex, $[(FF)FeCl]_2$ was dissolved in pyridine and subjected to a variable potential sweep cyclic voltammetry experiment. Over the potential range +0.50 to −1.30 V, only one process was observed at $E_{1/2} = 0.16$ V. The peak potential separation at slow potential sweep rates was that expected for a reversible one electron transfer. The difference between the peak potential and the potential at half peak current was also that expected for a one electron transfer process. Bulk electrolysis confirmed the passage of one electron per Fe atom in the complex. These results indicated that the presence of two non-interacting redox centers in this complex. The electrode reactant and product in the redox couple at $E_{1/2} = 0.16$ V were found to be spectrally identical to that observed [24] for $\{(TPP)Fe^{III}(py)_2\}^+$ and $(TPP)Fe^{II}(py)_2$, respectively.

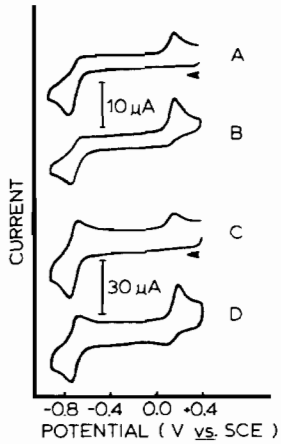

Fig. 5. Voltammetric data obtained on a 0.296 mM solution of $[(FF)Fe]_2O$ in pyridine. Traces A and B were recorded at a potential sweep rate of 1.00 V s^{-1}. Traces C and D were recorded at a potential sweep rate of 5.00 V s^{-1}. Traces A and C were first sweep cyclic voltammograms whereas traces B and D were steady state cyclic voltammograms.

In a third experiment, a solution containing $[(FF)FeCl]_2$ dissolved in pyridine was titrated with TBA^+OH^-. Addition of 1.0 eq of OH^- resulted in a decrease in the currents (both $i_{p,a}$ and $i_{p,c}$) for the redox couple at 0.16 V and the growth of a new reduction process at $E_{p,c} = -0.71$ V. At 2.0 eq of OH^-, the cathodic couple at $E_{p,c} = 0.13$ V had disappeared and the cathodic process at $E_{p,c} = -0.71$ shifted negatively. At 3.0 eq of OH^-, the voltammogram indicated complete conversion of $[(FF)FeCl]_2$ to $[(FF)Fe]_2O$. Comparable results were obtained if H_2O was used as the titrant instead of OH^-. A similar transformation from monomer to dimer were obtained when (TPP)FeCl was titrated with OH^-. However, addition of up to 30 eq of H_2O to pyridine solutions containing (TPP)FeCl did not produce voltammograms characteristic of the dimeric complex.

Spectroelectrochemistry of [(FF)Fe]$_2$O in Pyridine

A potentiostatic chronoabsorptometric experiment was carried out on a neat pyridine solution of [(FF)Fe]$_2$O. The spectrum of [(FF)Fe]$_2$O in pyridine was characterized by a Soret band at 412 nm and two visible bands at 572 and 611 nm. This spectrum remained unchanged over an applied potential of 1.30 to –0.55 V. Stepping the potential to –0.90 V resulted in immediate spectral changes. The Soret band underwent a 55% intensity increase and a 12 nm red shift. New visible bands appeared at 533 and 563 nm. The transition occurred with isosbestic points at 414, 449, 481 and 558 nm. This transition is shown in Fig. 6A. Reversing the potential to –0.55 V produced no changes in the electronic spectrum. In fact, no spectral changes were observed unless the applied potential was more positive than 0.0 V. At an applied potential of 0.40 V, a rapid spectral interconversion yielded the spectrum characteristic of [(FF)Fe]$_2$O within 60 s (see Fig. 6B). Bulk electrolysis at –0.90 V counted 2.13 ± 0.15 electrons per dimer being transferrred.

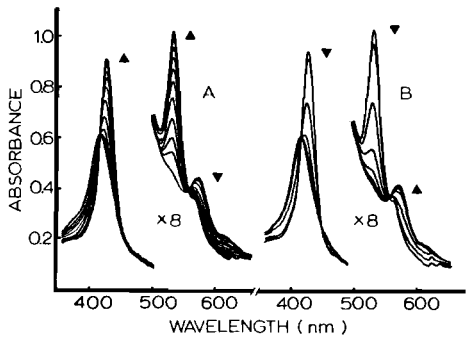

Fig. 6. Electronic spectra obtained during the electroreduction of a 0.494 mM solution of [(FF)Fe]$_2$O in pyridine. Part A depicts the spectra obtained when the applied potential was stepped from –0.55 to –0.90 V. Part B depicts the spectra obtained when the applied potential was stepped from 0.00 to 0.30 V. Spectra were acquired every 10 s.

Taken collectively, the combined voltammetric, coulometric and spectroelectrochemical results obtained for [(FF)Fe]$_2$O in pyridine can be best described by the following electron transfer sequence (eqns. (9)–(11)):

$$[(FF)Fe^{III}]_2O + 2e^- + 4py \xrightarrow{E \leq -0.71\,V} [(FF)Fe^{II}(py)_2]_2 + O^{2-} \quad (9)$$

$$[(FF)Fe^{II}(py)_2]_2 \xrightarrow{E \geq -0.16\,V} \{[(FF)Fe^{III}(py)_2]_2\}^{2+} + 2e^- \quad (10)$$

$$\{[(FF)Fe^{III}(py)_2]_2\}^{2+} + O^{2-} \xrightarrow{fast} [(FF)Fe^{III}]_2O \quad (11)$$

Reformation of the μ-oxo bridge between the two Fe centers is unique to the urea-linked dimer under these experimental conditions. When [(TPP)Fe]$_2$O was subjected to the identical spectroelectrochemical experiment as detailed above, electroreduction produced the monomeric (TPP)Fe^{II}(py)$_2$ species. Attempts to oxidatively reform the μ-oxo dimer (as observed for the urea-linked dimer) were totally unsuccessful.

We suggest that the unique reactivity of the urea-linked dimer in both solvent systems is a result of the strong hydrogen bonding ability of the urea-linkage. The X-ray crystal structure on this dimer [13] has shown that a water molecule is hydrogen bonded to both the oxygen atom bridging the two Fe centers and to the urea hydrogens. The $O_{bridging\,atom}$ to O_{water} distance was 2.81 and 2.87 Å and the O_{water} to $N_{urea\,linkage}$ distance was 2.86 and 2.82 Å*. These distances are consistent with reasonably strong hydrogen bonds [26]. Although this water molecule could be removed *in vacuo*, it is rapidly reinserted upon exposure to air of ambient humidity.

The involvement of the hydrogen bonded water molecule (in the urea-linked dimer) is manifested only by comparison of the redox reactivities of the two dimers. In $EtCl_2$, both dimers were electroreduced via an ECE sequence to produce a common product, the ferrous-hydroxy complex. Upon oxidation, the μ-oxo dimer is reformed for both porphyrins. However, the potential required to regenerate [(FF)Fe]$_2$O is ~400 mV anodic of that required for [(TPP)Fe]$_2$O. This potential shift is presumably due to the ability of the urea-linkage to stabilize the negatively charged {Fe^{II}–OH}$^-$ species through H-bonding between the urea hydrogens and the proton on the coordinated hydroxyl group. This parallels the reactivity observed for the amide-linked 'basket-handled' porphyrin [9c]. In pyridine, the influence of the urea-linkage is even more dramatic. For both porphyrins, electroreduction of the μ-oxo dimer yields the common product, Fe^{II}(py)$_2$. Oxidation of this species produced the ferric dipyridinated TPP derivative only, even in the presence of an excess of water. In contrast, oxidation of the pyridinated ferrous species of the urea-linked dimer resulted in the rapid reformation of the μ-oxo dimer. The water molecule, hydrogen bonded to the hydrophilic urea linkage, is in close proximity to the redox center. Upon oxidation, the central metals' affinity for coordinated solvent molecules diminishes. The increased charge on the central metal ions now attracts the water from the urea-linkage and initiates

*The water molecule took a major and minor position which were chemically indistinguishable. Consult ref. 13 for full details.

the dimerization sequence. The presence of the water molecule located in the dimer cavity through H-bonding to the urea-linkage also minimizes rotation of one porphyrin plane away from the other, ensuring the face-to-face conformation. The interaction of the water molecule and the urea-linkage, on one hand, and the interaction of the water molecule and the Fe centers on the other hand, provides control over the redox pathway for this hematin dimer, manifesting molecular environment effects in the redox chemistry of porphyrins possessing the NHCO functionality.

Acknowledgement

Acknowledgement is made to the National Institutes of Health (Grant No. HL33734-01) for support of this research.

References

1 (a) J. P. Collman, R. R. Gagne, T. R. Halbert, J. C. Marchon and C. A. Reed, *J. Am. Chem. Soc., 95,* 7868 (1973); (b) J. P. Collman and K. S. Suslick, *Pure Appl. Chem., 50,* 951 (1978) and refs. therein.
2 (a) J. Almog, J. E. Baldwin, R. L. Dyer and M. K. Peters, *J. Am. Chem. Soc., 97,* 226 (1975); (b) J. Almog, J. E. Baldwin, M. J. Grossley, J. F. DeBernardis, R. L. Dyer, J. R. Huff and M. K. Peters, *Tetrahedron 37,* 3589 (1981); (c) J. R Budge, P. E. Ellis, Jr., R. D. Jones, J. E. Linard, T. Szymanski, F. Basolo, J. E. Baldwin and R. L. Dyer, *J. Am. Chem. Soc., 101,* 4762 (1979).
3 (a) T. G. Traylor, *Acc. Chem. Res., 14,* 102 (1981) and refs. therein; (b) T. G. Traylor and P. S. Traylor, *Ann. Rev. Biophys. Bioeng., 11,* 105 (1982).
4 J. P. Collman, J. I. Braumann, T. J. Collins, B. L. Iverson and J. L. Sessler, *J. Am. Chem. Soc., 103,* 2450 (1981).
5 C. K. Chang, *J. Am. Chem Soc., 99,* 2819 (1977).
6 (a) A. R. Battersby, D. G. Buckley, S. G. Hartley and M. D. Turnbull, *J. Chem. Soc., Chem. Commun.,* 879 (1976); (b) A. R. Battersby, S. G. Hartley and M. D. Turnbull, *Tetrahedron Lett.,* 3169 (1978); (c) A. R. Battersby and A. D. Hamilton, *J. Chem. Soc., Chem. Commun.,* 117 (1980).
7 (a) M. Momenteau, B. Loock, J. Mispelter and E. Bisagni, *Nouv. J. Chim., 3,* 77 (1979); (b) M. Momenteau, J. Mispelter, B. Loock and E. Bisagni, *J. Chem. Soc., Perkin Trans I,* 189 (1983).
8 (a) M. Momenteau and D. Lavallette, *J. Chem. Soc., Chem. Commun.,* 341 (1982); (b) J. Mispelter, M. Momenteau, D. Lavalette and J. M. Lhoste, *J. Am. Chem. Soc., 105,* 5165 (1983).
9 (a) D. Lexa, M. Momenteau, P. Rentien, G. Rytz, J.-M. Saveant and F. Xu, *J. Am. Chem. Soc., 106,* 4755 (1984); (b) D. Lexa, P. Maillard, M. Momenteau and J.-M. Saveant, *J. Am. Chem. Soc., 106,* 6321 (1984); (c) D. Lexa, M. Momenteau, J.-M. Saveant and F. Xu, *Inorg. Chem., 24,* 122 (1985).
10 D. Chang, P. Cocolios, Y. T. Wu and K. M. Kadish, *Inorg. Chem., 23,* 1629 (1984).
11 A. Giraudeau, H. Callot and M. Gross, *Inorg. Chem., 18,* 201 (1979).
12 A. Giraudeau, H. J. Callot, J. Jordan, I. Ezhar and M. Gross, *J. Am. Chem. Soc., 101,* 3857 (1979).
13 J. T. Landrum, D. Grimmett, K. J. Haller, W. R. Scheidt and C. A. Reed, *J. Am. Chem. Soc., 103,* 2640 (1981).
14 (a) A. D. Adler, F. R. Longo, J. D. Finarelli, J. Goldmacher, J. Assour and L. Korsakoff, *J. Org. Chem., 32,* 476 (1967); (b) A. D. Adler, F. R. Longo, F. Kampas and J. Kim, *J. Inorg. Nucl. Chem., 32,* 2443 (1970).
15 L. A. Bottomley, M. R. Deakin and J.-N. Gorce, *Inorg. Chem., 23,* 3563 (1984).
16 R. L. Birke, M.-H. Kim and M. Strassfeld, *Anal. Chem., 53,* 852 (1981).
17 P. Zuman, 'Substituent Effects in Organic Polarography', Plenum, New York, 1967.
18 K. M. Kadish, G. Larsen, D. Lexa and M. Momenteau, *J. Am. Chem. Soc., 97,* 282 (1975).
19 (a) M. A. Phillippi, E. T. Shimomura and H. M. Goff, *Inorg. Chem., 20,* 1322 (1981); (b) M. A. Phillippi and H. M. Goff, *J. Am. Chem. Soc., 104,* 6024 (1982); (c) E. T. Shimomura, M. A. Phillippi and H. M. Goff, *J. Am. Chem. Soc., 103,* 6778 (1981); (d) M. A. Phillippi and H. M. Goff, *J. Am. Chem. Soc., 101,* 7641 (1979).
20 S. A. Wenk and F. A. Schultz, *J. Electroanal. Chem., 101,* 89 (1979).
21 S. E. Jones, G. S. Srivastava, D. T. Sawyer, T. G. Traylor and T. C. Mincey, *Inorg. Chem., 22,* 3903 (1983).
22 R. H. Felton, G. S. Owen, D. Dolphin, A. Forman, D. C. Borg and J. Fajer, *Ann. N.Y. Acad. Sci., 206,* 504 (1973).
23 A. Wolberg, *Isr. J. Chem., 12,* 1031 (1974).
24 L. A. Bottomley, R. K. Rhodes and K. M. Kadish, in C. Ho (ed.), 'Interaction Between Iron and Proteins in Oxygen and Electron Transport', Elsevier, New York, 1982, p. 117.
25 L. A. Bottomley, C. Ercolani, J.-N. Gorce, G. Pennesi and G. Rossi, *Inorg. Chem., 25,* 2338 (1986).
26 W. C. Hamilton and J. A. Ibers, in 'Hydrogen Bonding in Solids', Benjamin, New York, 1968.